



Evaluation of Silica Fume on the Performance of Corroded Concrete with Bacteria Using NDT Methods

Ahmad Zaki ^{1,2,*} ; Muhammad Restu Riady Putra ¹; Sri Atmaja P. Rosyidi ¹; Abdullah M. Zeyad ³; Kharisma Wira Nindhita ²

1. Department of Civil Engineering, Universitas Muhammadiyah Yogyakarta, Bantul 55183, Special Region of Yogyakarta, Indonesia

2. Magister of Civil Engineering, Universitas Muhammadiyah Yogyakarta, Bantul 55183, Special Region of Yogyakarta, Indonesia

3. Civil and Architectural Engineering Department, College of Engineering and Computer Sciences, Jazan University, Jazan 45142, Saudi Arabia

* Corresponding author: ahmad.zaki@umy.ac.id

ARTICLE INFO

Article history:

Received: 04 February 2025

Revised: 25 April 2025

Accepted: 17 August 2025

Keywords:

Silica Fume,
Bacteria,
Concrete,
Corrosion,
NDT.

ABSTRACT

Silica fume can be used in place of cement to make reinforced concrete more resistant to corrosion. Cracks and corrosion can also be treated using *Bacillus subtilis* bacteria added to the mix. Using non-destructive testing, this study intends to ascertain the effects of silica fume addition to concrete bacteria on the mechanical and corrosion characteristics of the material. The beams and cylinders used in the tests were 50 x 10 x 10 cm³ and 30 x 15 cm³, respectively. In place of cement, the specimens had 8%, 10%, and 12% silica fume, and 10 ml (10⁵ cfu/ml) of *Bacillus subtilis* bacteria were added. The direct current power supply is used in the accelerated corrosion process for 48, 96, and 168 hours. Regarding compressive strength, the typical concrete specimen tested at 37.59 MPa was the strongest. Silica fume concrete outperforms regular concrete in the flexural strength test. Compared to regular concrete, superior results were obtained from non-destructive tests conducted on silica fume concrete utilizing impact echo and resistivity instruments. The longer the concrete is exposed to corrosion, the lower the impact echo and resistivity values that are subsequently measured. By accelerating the corrosion process of silica fume concrete by 48, 96, and 168 hours, respectively, the impact echo and resistivity values for corrosion resistance reached their maximums of 12%, 10%, and 8%.

E-ISSN: 2345-4423

© 2025 The Authors. Journal of Rehabilitation in Civil Engineering published by Semnan University Press.

This is an open access article under the CC-BY 4.0 license. (<https://creativecommons.org/licenses/by/4.0/>)

How to cite this article:

Zaki, A, Riady Putra, M. R, Rosyidi, S. A. P., Zeyad, A. M. and Nindhita, K. W. (2026). Evaluation of Silica Fume on the Performance of Corroded Concrete with Bacteria Using NDT Methods. Journal of Rehabilitation in Civil Engineering, 14(2), 2266. <https://doi.org/10.22075/jrce.2025.2266>

1. Introduction

The increasing demand for concrete will lead to carbon dioxide (CO₂) emissions from the production of cement, which can threaten human health and have a negative impact on the environment [1]. The statement shows that it is necessary to take measures to prevent the increase of CO₂ emissions by reducing the main elements of concrete using green concrete from waste utilization such as fly ash (FA), silica fume (SF) [2], rice husk ash (RHA), recycled coarse aggregate (RCA), and others [3]. SF is one of the materials that can be used as a substitution component for concrete cement. SF has many advantages, such as reduced CO₂ emissions, cost-effectiveness, improved durability, and mechanical properties of concrete [4]. Adding SF in concrete due to the reaction of silicon dioxide (SiO₂), which takes calcium hydroxide (CH) from cement hydration, will reduce the permeability and porosity of concrete. SF can inhibit corrosion and reduce the corrosion rate after the corrosion reaction has started, depending on the correct proportion of SF mixture [5]. However, adding SF to concrete still has the possibility of corrosion if the concrete is exposed to extreme environments [6].

One of the main factors of structural damage is corrosion. Steel corrosion in concrete can be a serious problem due to its frequent occurrence in certain types of structures and the high cost of repairing such structures. Concrete has a highly alkaline environment, which results in the formation of a passivity layer that protects steel reinforcement from corrosion. However, this protective layer will be damaged if the concrete is not durable [7]. The main factors of corrosion are exposure of reinforced concrete (RC) to chlorides and carbonation of concrete or other exposure conditions that reduce the alkalinity of concrete ACI 222R-19 (ACI, 2019). In the research of Patil et al. [8], rusting of reinforcement concrete's durability and strength will be impacted because steel reinforcement can expand to many times its original size, causing significant pressure within the concrete. This pressure may lead to cracking, delamination of the concrete surface, and exposing the reinforcement to additional corrosion activity. Corrosion of steel reinforcement in concrete can damage the concrete body and reduce the concrete's service ability [9]. In construction, new solutions to the problem of corrosion-induced fracture damage in concrete are emerging. Self-healing concrete (SHC) is the addition of microorganisms to the concrete mixture that can repair cracked concrete. One of the microorganisms used in the SHC method is *Bacillus subtilis*, which can fill voids, pores, and micro-cracks due to the effectiveness of bacteria in depositing a layer of Calcium Carbonate (CaCO₃) [10]. In tests conducted by Nguyen et al. [11] found that the addition of *Bacillus subtilis* to concrete lowers its porosity and increases its compressive strength. This is because bacterial metabolism leads to microbial precipitation. Concrete can be protected against corrosion caused by CaCO₃ deposits by *Bacillus subtilis* bacteria, which can also repair gaps in the material by decreasing porosity and plugging pores, making the material denser.

In some studies, using SF and bacteria can significantly reduce concrete porosity and inhibit chloride ion penetration. The reduction in concrete porosity results from the SF pozzolanic reaction that makes the concrete microstructure denser and bacteria that precipitate calcite in the concrete pores [12]. Increasing the percentage of the SF mixture can reduce the level of penetration of chloride ions in concrete so that the concrete's resistance to extreme environments such as seawater becomes better. However, the increasing percentage of SF will decrease the workability of concrete, which is due to the characteristic of SF that absorbs water from the small particle size of SF [13]. Tests conducted by Grazulyte et al. [14], to comprehensively investigate the effect of SF at percentages of 0%, 7%, and 10% with additives such as superplasticizers on the performance of high-strength concrete proved a significant improvement in concrete performance in terms of compression, tension, and flexure. Nguyen et al. [11] conducted tests using *Bacillus subtilis* bacteria to determine compressive strength, porosity, water absorption, and chloride permeability at 28 and 90 days of concrete age. The test used a concentration of bacillus subtilis bacteria of 10⁵ cells/ml and found that bacillus subtilis bacteria were able to increase compressive strength and reduce porosity and chloride permeability of concrete. Calcite precipitation by *Bacillus subtilis* bacteria fills the

pores, reduces porosity, and makes the concrete denser. CaCO_3 precipitation on the surface and pores of the concrete microstructure results in decreased water absorption and porosity. As a result, chloride penetration is reduced and can reduce the potential for concrete reinforcement corrosion. Bacteria will grow as water penetrates through the concrete's fractures and finally turn into limestone. The concrete surface fractures will be filled up and sealed by the limestone when it hardens [15]. The addition of SF and bacteria, which can reduce porosity and make concrete denser, can reduce the potential for corrosion in concrete [16]. A study examining the effects of reinforcement corrosion on the flexural strength of reinforced concrete beams caused by a 10.5% NaCl solution revealed that the corrosion led to a drop in the flexural strength, tensile strength, and weight of the reinforcement.

Besides the development of concrete mixture technology, evaluation technology for structures is also growing. Structural assessment techniques using non-destructive testing (NDT) methods are used to inspect corroded reinforced concrete without damaging the structure [17,18]. NDT procedures are preferred since they inflict minimal or no harm to the existing concrete while evaluating the condition of corroded concrete [19]. Zaki et al. [20] researched to investigate the influence of corrosion levels on oil palm shells (OPS) and fiber mask concrete. The research utilized the NDT approach, employing resistivity and impact echo equipment. The study employed accelerated corrosion by submerging concrete specimens in a 5% NaCl solution and utilizing a direct current (DC) power supply. After accelerating the corrosion, this study tested using NDT methods, namely, resistivity and impact-echo, to analyze and detect the effect of corrosion. It was found that the resistivity and the impact echo values will decrease as the corrosion level increases.

Research on the evaluation of silica fume on the self-healing performance of corroded concrete using the NDT method remains limited. The combination of silicafume and bacteria has the potential to significantly reduce corrosion and its effect. Evaluation using the NDT method is used to determine the condition of the concrete due to corrosion without causing further damage. Therefore, this study focus on investigating the performance of self-healing concrete incorporating SF and bacteria under accelerated corrosion conditions, assessed through NDT method. This analysis include measurements of compressive strength, flexural strength, impact echo, and resistivity values before and after corrosion. Additionally, this study examines corrosion rate based on Faraday's law, the reduction of reinforcement diameter, crack width, and visual self-healing observations on corroded and cracked concrete.

2. Methodology

2.1. Materials

The fine aggregate (sand) material used in this study came from Progo River Yogyakarta, while the coarse aggregate (gravel) was from Clereng Yogyakarta. The specimens were made using PCC cement from Dynamix with Ø12 mm steel reinforcement and 60 cm length with specimen size of 50 cm x 10 cm x 10 cm. The silica fume material was obtained from Sika Indonesia company, while the self-healing bacteria-based *Bacillus subtilis* was cultivated at the Agrobiotechnology Laboratory, Faculty of Agriculture, Universitas Muhammadiyah Yogyakarta. The value of the fine aggregate test results is presented in Table 1. These results have met the required standards. Table 2 shows the test results for the coarse aggregate. The coarse aggregate results also meet the specified requirements. Both sets of results are essential for evaluating the overall material quality.

Table 1. Fine aggregate test data.

Test Type	Value	Unit	Standard
Fine modulus	2.435	-	SNI ASTM C136:2012 [21]
Bulk specific gravity	1.837	-	SNI 1970:2008 [22]
Saturated surface dry specific gravity	2.242	-	SNI 1970:2008 [22]
Apparent specific gravity	3.094	-	SNI 1970:2008 [22]
Water absorption	22.165	%	SNI 1970:2008 [22]
Mud content	1.00	%	SNI ASTM C117:2012 [23]

Table 2. Coarse aggregate data.

Test Type	Value	Unit	Standard
Bulk specific gravity	2.642	-	SNI 1969:2008 [24]
Saturated surface dry specific gravity	2.707	-	SNI 1969:2008 [24]
Apparent specific gravity	2.826	-	SNI 1969:2008 [24]
Water absorption	2.459	%	SNI 1969:2008 [24]
Mud content	1.00	%	SNI ASTM C117:2012 [23]
Abrasion	15.75	%	SNI 2417:2008 [25]

2.2. Mix design

Concrete mix planning using ACI 211.1-91 of 2002 on the procedure for maintaining proportions to manufacture normal concrete [26]. The planned concrete quality was 30 MPa. Cement was replaced with silica fume proportion of 0%, 8%, 10%, and 12%, while self-healing bacteria *Bacillus subtilis* used proportion (10^5 cfu/mL) with 10 ml bacteria per specimen. The specimen code for normal concrete is marked with BN, while concrete with a mixture of 8% silica fume is marked SFB8, 10% silica fume concrete is marked SFB10, and concrete with 12% silica fume is marked with SFB12. Mix design per 1 m³ can be seen in Table 3. The optimum silica fume content in concrete mix design is typically around 10% by weight of cement, balancing strength, durability, and workability. A 2000 mL suspension of bacteria was used to partially replace mixing water, based on prior studies and preliminary trials indicating this volume ensures effective bacterial distribution and activity without compromising concrete workability. This amount corresponds to approximately 10% of the total mixing water, aligning with typical dosages in self-healing concrete research.

Table 3. The proportion of mix design of concrete test specimens 1 m³

Materials	Total				Units
	BN	SFB8	SFB10	SFB12	
Water	205	205	205	205	liter
Cement	484.213	445.476	435.791	426.107	kg
Fine aggregate	641.398	641.398	641.398	641.398	kg
Coarse aggregate	984.75	984.75	984.75	984.75	kg
Silica fume	-	38.737	48.421	58.105	kg
Bacteria	2000	2000	2000	2000	ml

2.3. Preparations materials

The specimens were made with a size 50 cm x 10 cm x 10 cm beams and 15 cm x 30 cm cylinders. The size of the main reinforcement is Ø12 mm. A cable is connected to the end of the reinforcement to serve as a conduit for the process of accelerating concrete corrosion, facilitated by a DC power supply. Test specimens were made based on the proportion of bacteria mixture with 10^5 cfu/ml water and silica fume at 0%, 8%, 10%, and 12%. The bacteria used in the name are *Bacillus subtilis*. *Bacillus subtilis* bacteria were obtained from the Agrobiotechnology Laboratory, Faculty of Agriculture, Universitas Muhammadiyah Yogyakarta. This strain is a Gram-positive, endospore-forming, rod-shaped bacterium widely known for its ability to precipitate calcium carbonate through microbial-induced calcite precipitation (MICP), making it suitable for self-healing concrete applications. The bacteria were cultured in a nutrient-rich medium under controlled laboratory conditions to reach the required cell concentration before incorporation into the concrete mixture. No commercial purchase was made; instead, the strain was isolated and propagated in-house, which significantly reduced the research cost. The bacteria were mixed during the mixing of fresh concrete.

The concrete that has been mixed will be tested for looseness during the concrete-making process by testing the slump value. After the slump test, the concrete mixture was poured into the formwork until it was full

and solid so that no air voids formed. Then, the concrete is allowed to harden for 24 hours, removed from the formwork and weighed. A sketch of the test specimen can be seen in Fig 1. Slump testing is conducted to ascertain the viscosity level of the concrete that will be utilized. The slump test results are expressed in cm using Abrams's cone and pounding stick (SNI 2493:2011) [27]. This study planned the slump value to be 7.5-10 cm. After 24 hours, the mold of the specimen was removed, and the test specimens were placed at the curing site. Concrete curing is a treatment process by soaking after the concrete is cast and the mold is opened to keep the concrete from losing water too quickly, maintain moisture, and maintain the temperature in the concrete so that the hydration process can run perfectly [28].

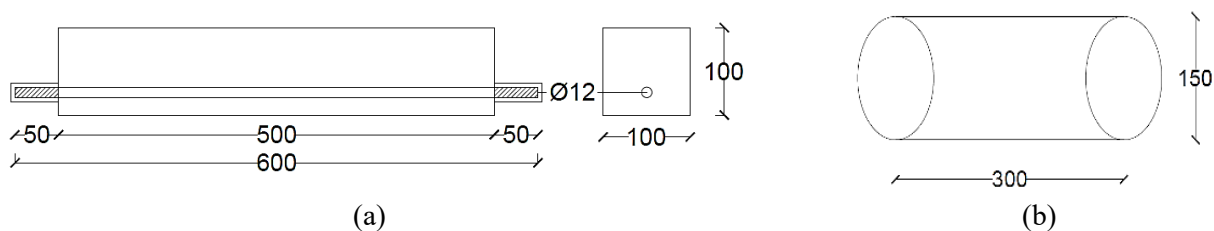


Fig. 1. Specimens: (a) Beams and (b) Cylinders (in mm).

2.4. Non-destructive testing (NDT)

Steel reinforcement corrosion has emerged as a primary factor contributing to structural failures. Non-destructive testing (NDT) has demonstrated its use in the detection and evaluation of corrosion-induced damage in reinforced concrete (RC) structures [29]. With this method, the evaluation of concrete against corrosion is more effective. This research will utilize NDT with resistivity and impact echo tools. Resistivity testing was carried out when the test specimens were 28 days old. This test is carried out before and after the accelerated corrosion process to compare the test results of the corrosion process. For the data obtained to be complete and more accurate, the resistivity measurement tool uses the Four Point Probe method, which is carried out three times at each point so that the data obtained is complete and more accurate. This test uses the parameters determined by AASHTO TP 95 [30]. Details of the division of points carried out by resistivity testing are provided in Fig. 2. The figure illustrates the specific points used for testing. These points were carefully chosen based on the resistivity characteristics of the material. Each point corresponds to a different area of the sample tested. The results from these points help in analyzing the overall resistivity performance.

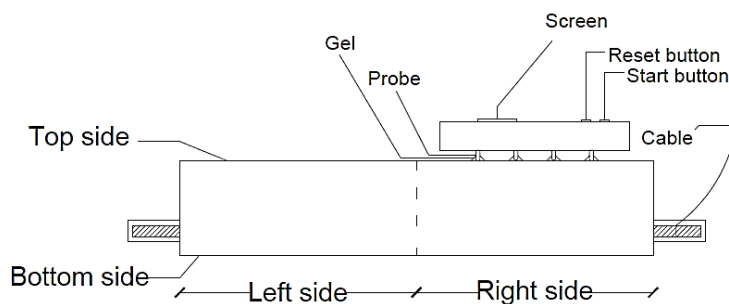


Fig. 2. Resistivity testing illustration.

Impact Echo testing was carried out when the object was 28 days. This test was conducted before and after the accelerated corrosion process to compare the test results using the parameters that have been determined by ASTM C1383 [31]. The impact-echo method is a methodology used to identify flaws or imperfections in concrete structures. It relies on observing surface displacement caused by immediate mechanical force. The concrete will be subjected to many taps using an impact echo test instrument, after which the sensor will detect the signal at a pre-determined distance from the impact location. Impact echo testing was

conducted with two sensors at the hit points of 5 cm, 10 cm, 15 cm, and 20 cm. Details of impact echo testing at each distance can be seen in Fig 3. This method allows for a precise analysis of the concrete's internal condition. The data gathered helps in evaluating the material's integrity and identifying any potential flaws.

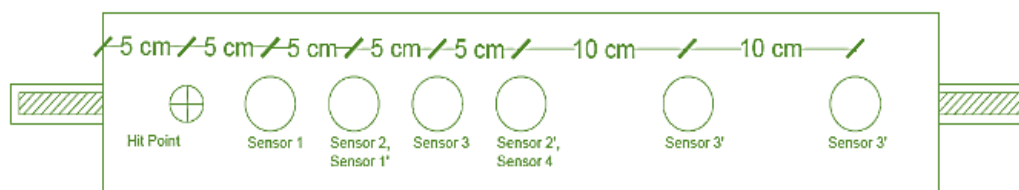


Fig. 3. Details of impact echo testing at each distance.

2.5. Acceleration corrosion

Accelerated corrosion testing may be designed based on Faraday's Law, which quantifies the percentage decrease in the reinforcement mass caused by corrosion [32]. The procedure and formula used are based on ASTM STP866-EB for Laboratory Corrosion Tests and Standards [33]. Accelerated corrosion of the test specimens is required because the natural corrosion process takes a long time. The steel reinforcement in concrete is corroded using a DC power supply to accelerate the corrosion process, and the duration and use of electric current can be adjusted as needed. The reinforcing steel was connected to the positive pole (+) as the anode and the other reinforcing steel to the negative pole (-) as the cathode. The corrosion process was conducted for 48, 96, and 168 hours. Concrete reinforcement was wired on one side to be connected to the positive pole of the DC power supply. Then, the concrete was immersed in a saline solution with 5% salinity. The corrosion acceleration sketch and scheme can be seen in Fig 4.

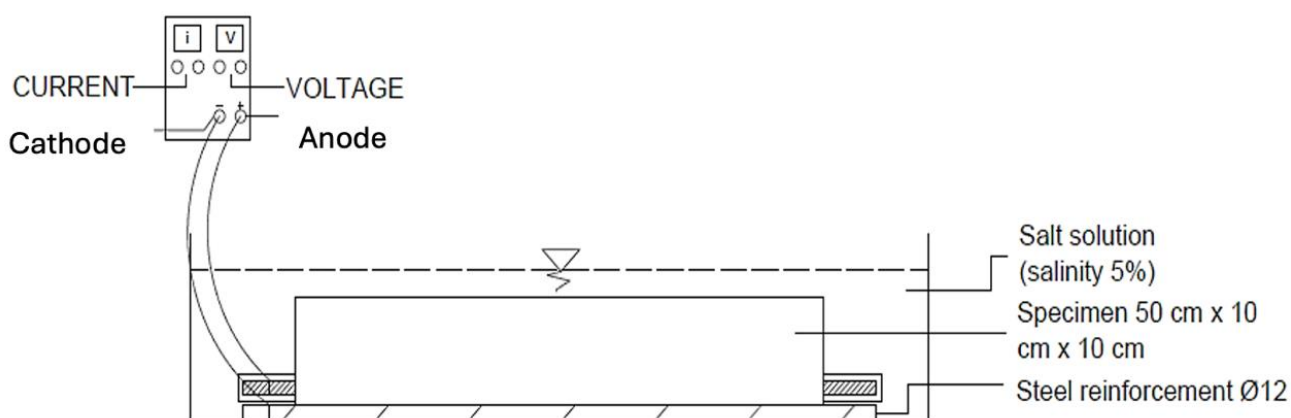


Fig. 4. Sketch of accelerated corrosion testing.

2.6. Compressive and flexural strength

The experiment was carried out on concrete cylinders that had been immersed in water for 28 days. A Universal Testing Machine (UTM) is used to measure the compressive strength of test specimens in concrete mixes, utilizing SF and bacteria. The procedure and test result are calculated using the standard SNI 1974:2011 [34]. The flexural strength of the test specimens was assessed using a Universal Testing Machine once the corrosion process had concluded. The Structures and Construction Materials Laboratory of the Civil Engineering Department of Universitas Muhammadiyah Yogyakarta conducted testing to determine the flexural strength of concrete. Concrete beams' procedure and test results are calculated using standards based on SNI 4154:2014 [35]. The experiment was conducted by placing a single weight at the midpoint of the beam's span, with a 5 cm gap between the support and the beam's edge. This test aimed to ascertain the flexural strength of corroded beams at various proportions of silica fume and bacteria mixture.

3. Results and discussion

3.1. Compressive strength

Concrete cylinders were subjected to compressive strength testing after 28 days of curing. The results, illustrated in Fig. 5, show the control beam (BN) achieved an average compressive strength of 37.59 MPa. The concrete incorporating 8% silica fume exhibited an compressive strength of 33.99 MPa. However, increasing silica fume to 10% and 12% reduced the strength to 24.10 MPa and 29.92 MPa. Fig 5 demonstrates that BN concrete has a greater compressive strength than Silica Fume concrete. This reduction can be attributed to the lower reactivity of excessive silica fume, which limits its interaction with water and cement. This leads to a decrease in the amount of water available for compacting the concrete, resulting in the formation of voids. Furthermore, a higher percentage of silica fume added to the concrete only serves as a filler in the space between the cement paste and the aggregate, decreasing compressive strength [36]. During the process of hydration, the chemical reaction between cement and water forms calcium silicate hydrate (CSH) and calcium hydroxide. The creation of CSH influences the compressive strength of concrete, and the quantity of CSH created is strongly contingent upon the quantity of cement utilized [37]. Increasing the amount of silica fume may result in a portion of the residual silica fume not undergoing a reaction with calcium hydroxide, thus failing to create CSH gel. Instead, it would simply fill the empty spaces between the cement paste and the aggregate [38].

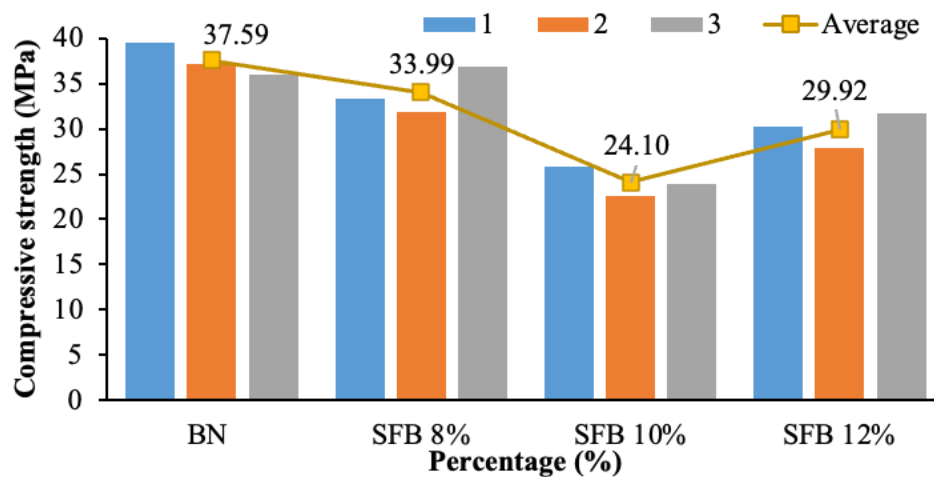


Fig. 5. Concrete compressive strength test results.

3.2. Corrosion acceleration

Beam specimens that had undergone a 28-day curing process were subjected to acceleration testing. The specimens were submerged in a solution of Sodium Chloride (NaCl) with a salinity of 5% of the total volume of water in the styrofoam. A DC power supply tool assisted in the corrosion acceleration process to provide electric current to the reinforcement of the test specimens. Accelerated corrosion was carried out using a duration of 48 hours, 96 hours, and 168 hours on 12 beams of test specimens, and the current was read every hour to see the increase in current on each test specimen. In Fig 6, the results show that concrete with SFB admixture has a relatively small current compared to normal concrete. The concrete with SFB admixture exhibits a relatively small current. This indicates that the admixture affects the conductivity of the concrete. Compared to normal concrete, which shows a higher current, the SFB admixture reduces the electrical flow. This difference highlights the impact of the admixture on the material's electrical properties.

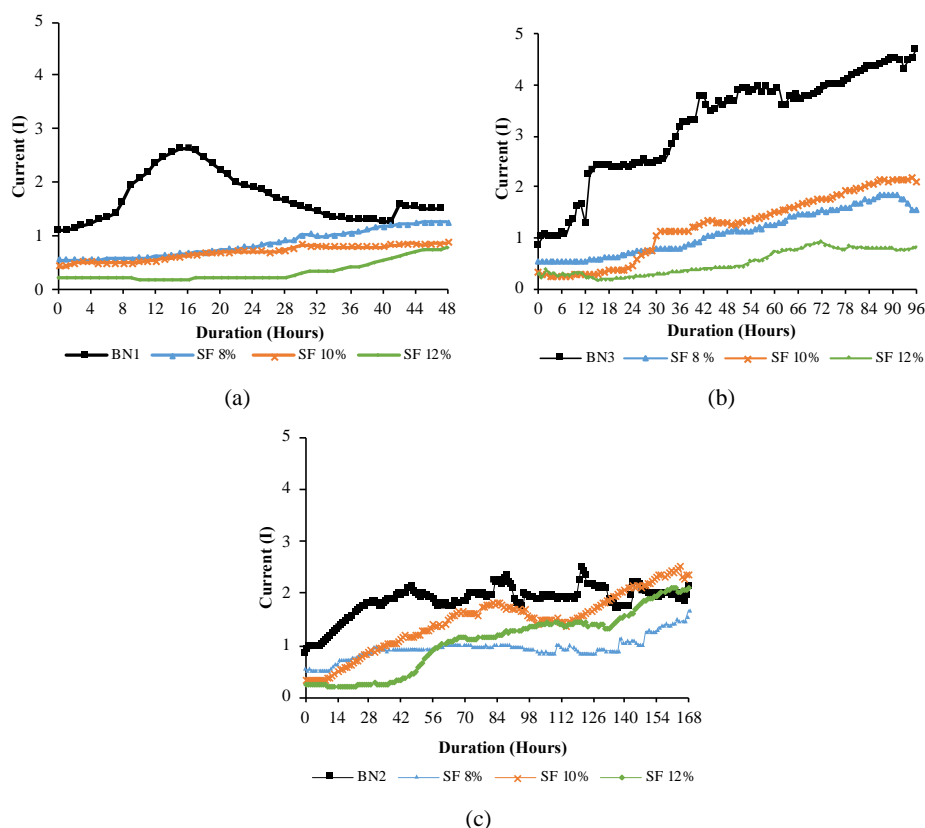


Fig. 6. Corrosion acceleration graph (a) 48 hours, (b) 96 hours, and (c) 168 hours.

The current was monitored every hour to record the average intensity of the corrosion current flowing through the specimens at different concrete mixes. This increase in current explains the resistance of concrete to chloride initiation. At accelerated corrosion with 48 48-hour duration, SFB 12% had lower initial to final current values, followed by SFB 10%, SFB 8%, and BN concrete mixes. At 96 hours, SFB 12% still had low initial to final currents, followed by SFB 8%, SFB 10%, and BN. At a corrosion acceleration duration of 168 hours, SFB 8% had a lower initial to final current, followed by SFB 12%, SFB 10%, and BN. This proves that SF and bacterial admixture concrete have lower current than normal concrete, which indicates that silica fume and bacterial admixture concrete have better resistance than normal concrete. After the accelerated corrosion process, it is possible to calculate the estimated final weight of the reinforcement and the estimated mass loss from the average current obtained during the accelerated process with the impressed voltage method. The estimated mass loss of the reinforcement due to the corrosion process can be seen in Table 4.

Table 4. Calculation of estimated reinforcement weight loss.

Code	Current (I)	Acceleration duration (hours)	Initial Weight (gr)	Estimated Weight Final (gr)	Estimation Rate Corrosion (%)	Estimation Mass Loss (gr)
BN1	1.70	48	500	414.96	17.01	85.03
BN2	1.84	168	500	177.98	64.40	322.02
BN3	3.25	96	500	173.87	65.23	326.13
SFB 8%A1	0.86	48	500	457.13	8.57	42.87
SFB 8%A2	1.13	96	500	386.24	22.75	113.76
SFB 8%A3	0.95	168	505	338.67	33.94	166.33
SFB 10%B1	0.69	48	500	465.56	6.89	34.44
SFB 10%B2	1.28	96	490	362.10	25.58	127.90
SFB 10%B3	1.45	168	490	234.72	52.10	255.28
SFB 12%C1	0.34	48	500	483.15	3.37	16.85
SFB 12%C2	0.55	96	500	444.75	11.05	55.25
SFB 12%C3	1.06	168	490	303.18	38.13	186.82

Table 5 displays the data on mass loss and the percentage of real corrosion rate. Pitting corrosion can occur due to chloride ions present on the reinforcing surface or the penetration of water and oxygen into certain areas of the concrete that include cracks, leading to a decrease in cross-sectional area. Pitting corrosion can lead to a fast reduction in the cross-sectional area of the reinforcement in specific crucial regions [39]. The reduction in the cross-sectional area in this investigation was recorded at intervals of 5 cm along the reinforcement. Figure 7 displays the outcomes of the cross-sectional area measurement. From the measurement results, it was found that corrosion can cause a reduction in the cross-sectional area of the reinforcement. The higher the corrosion rate, the more reduction in the cross-sectional area of the reinforcement [40]. From the graph in Fig 7, BN has more reduction in cross-sectional area than SFB, which means that concrete with added silica fume and bacteria can minimize the reduction in the cross-sectional area of the reinforcement, which will cause a decrease in the adhesion between the reinforcement. In addition, the strength of the concrete will be reduced due to the decrease in the adhesion of the reinforcement to the concrete.

Table 5. Reinforcement mass loss.

Code	Final Weight (gr)	Estimation Rate Corrosion (%)	Rate Corrosion Actual (%)	Estimates Mass Loss (gr)	Mass Loss Actual (gr)	Derivation (%)
BN1	454	17.01	9.20	85.03	46.00	7.81
BN2	287	64.40	42.60	322.02	213.00	21.80
BN3	327	65.23	34.60	326.13	173.00	30.63
SFB 8%A1	490	8.57	2.00	42.87	10.00	6.57
SFB 8%A2	428	22.75	14.40	113.76	72.00	8.35
SFB 8%A3	396	32.94	21.58	166.33	109.00	11.35
SFB 10%B1	492	6.89	1.60	34.44	8.00	5.29
SFB 10%B2	411	26.10	16.12	127.90	79.00	9.98
SFB 10%B3	301	52.10	38.57	255.28	189.00	13.53
SFB 12%C1	495	3.37	1.00	16.85	5.00	2.37
SFB 12%C2	465	11.05	7.00	55.25	35.00	4.05
SFB 12%C3	365	38.13	25.51	186.82	125.00	12.62

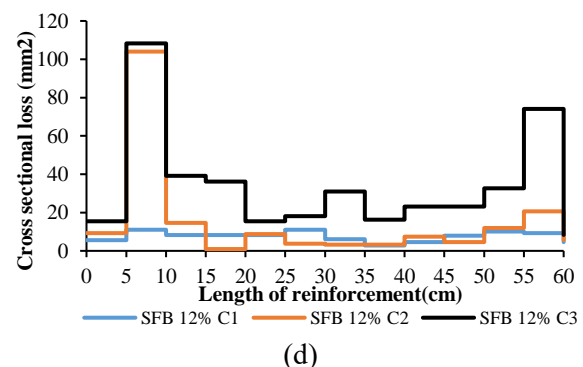
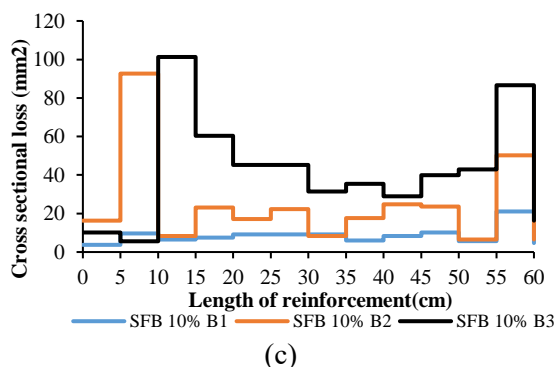
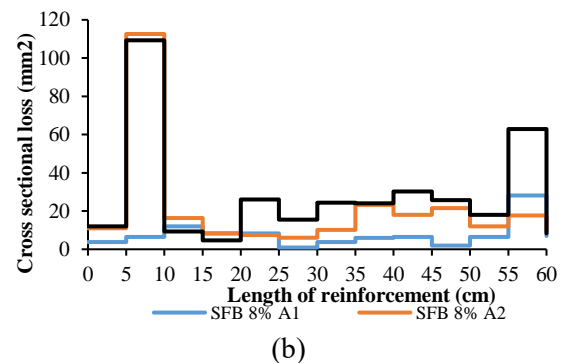
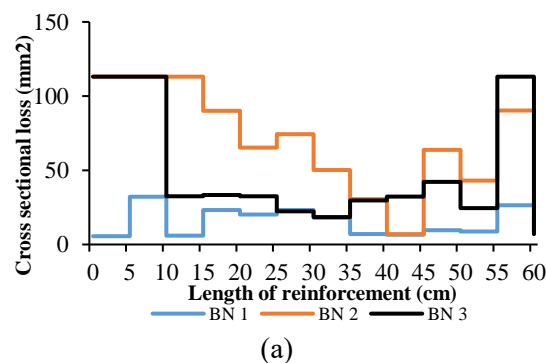


Fig. 7. Measurement results of reduction of reinforcement cross-sectional area (a) BN, (b) SFB 8%, (c) SFB 10%, and (d) SFB 12%.

The acceleration results show that the longer the accelerated corrosion process, the higher the mass loss of reinforcement, which aligns with the estimated value not too far from the actual value by not exceeding 30.63%. The accelerated corrosion test runs quite controlled, with the correlation between the duration of accelerated corrosion and the actual corrosion rate above 90%, as can be seen in Fig 8. The value of 30.63% is the highest derivation value obtained by BN 3, and this occurs because, during the accelerated corrosion process, BN 3 has been set for a duration of 168 hours. However, at 13 hours, BN 3 experienced initial cracking and increased current on BN 3 so that chloride penetration became high, which affected the derivation value. Sudden spikes in current indicate the formation of early corrosion cracks in concrete [41].

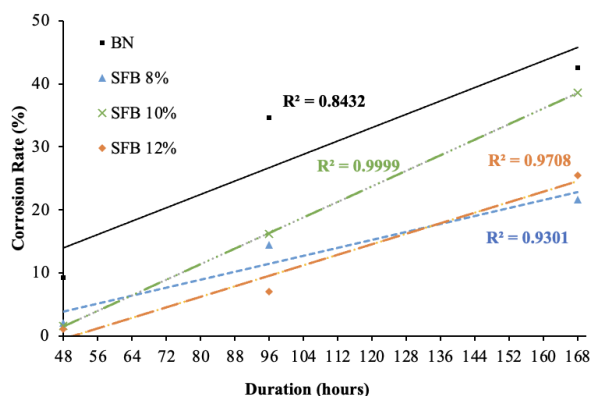


Fig. 8. Relationship between corrosion duration and corrosion rate.

From the results of accelerated corrosion over a predetermined time, it is known that at 48 hours of corrosion acceleration, SFB 12% C1 has a low average current compared to other specimens with a current acquisition of 0.34 (I), making SFB 12% C1 has good resistance at 48 hours duration this is evidenced from the actual corrosion rate of 1% with actual mass loss of 5 grams. At 96 hours of corrosion acceleration, SFB 12% C2 has an average current of 0.55 (I), making SFB 12% C2 have good resistance at 96 hours of corrosion acceleration duration with an actual corrosion rate of 7% and actual mass loss reduction of 35 grams. At 168 hours of accelerated corrosion, SFB 8% A3 had good resistance with an average current of 1.45 (I), a corrosion rate of 21.58%, and a mass loss of 109 grams. The best corrosion resistance of each specimen in 48 hours and 96 hours duration is SFB 12%, while 168 hours is SFB 8%, which makes SFB 8% have good resistance in the long term compared to other specimens. There are cracks due to corrosion formation after the accelerated corrosion process on the specimen. The width of cracks in the specimens have different sizes because the accelerated corrosion process is highly dependent on the permeability and water absorption of concrete to chloride penetration [41]. The results of cracking due to the accelerated corrosion process of 168 hours corrosion can be seen in Fig 9, while the results of crack measurements can be seen in Table 6.

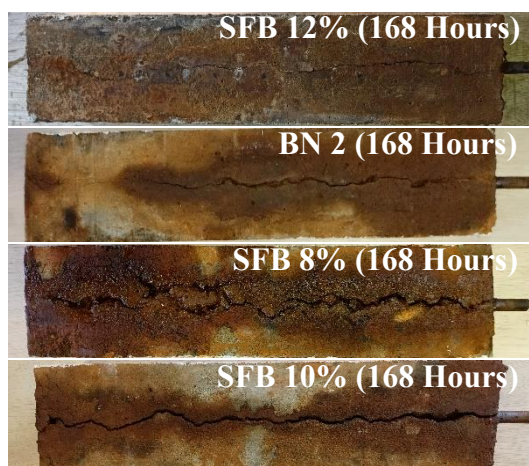
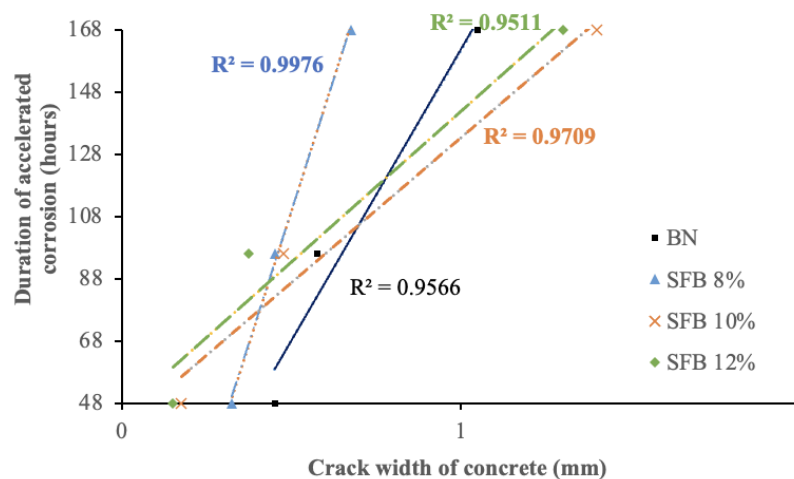


Fig. 9. Concrete cracks after an accelerated corrosion process of 168 hours.

Table 6. Crack measurement.

Code	Acceleration Duration Corrosion (Hours)	Corrosion Crack Width (mm)		Average
		Left	Right	
BN1	48	0.30	0.60	0.45
BN2	168	0.70	1.40	1.05
BN3	96	0.40	0.75	0.58
SFB 8%A1	48	0.35	0.30	0.33
SFB 8%A2	96	0.55	0.35	0.45
SFB 8%A3	168	0.90	0.45	0.68
SFB 10%B1	48	0.20	0.15	0.18
SFB 10%B2	96	0.50	0.45	0.48
SFB 10%B3	168	1.40	1.40	1.40
SFB 12%C1	48	0.20	0.10	0.15
SFB 12%C2	96	0.40	0.35	0.38
SFB 12%C3	168	1.30	1.40	1.35

From the measurement of cracks in all specimens, the average is taken on the right and left sides, which can be seen, for example, in Fig 10. It is known that the longer the duration of corrosion, the greater the crack width. The longer the duration of accelerated corrosion, the more rust products will increase and collect on the steel surface [42]. The corrosion of steel reinforcement in concrete has a detrimental impact on its durability and strength. This is due to the potential of the steel reinforcement to undergo significant expansion, resulting in high pressure within the concrete. Consequently, this pressure leads to the formation of cracks [8]. In Fig 10, the relationship between the duration of accelerated corrosion and crack width correlates > 90%, which explains that the duration of corrosion and crack width in concrete are closely related.

**Fig. 10.** Relationship between accelerated corrosion duration and crack width.

3.3. Non-destructive testing

3.3.1. Impact echo

Impact echo testing is a method to determine the gap or cavity in a concrete structure layer. Impact echo testing was carried out at four concrete points before and after corrosion with different distances of 5 cm, 10 cm, 15 cm, and 20 cm from the Hit point with three iterations. Examples of impact echo testing graphs before and after corrosion can be seen in Fig 11.

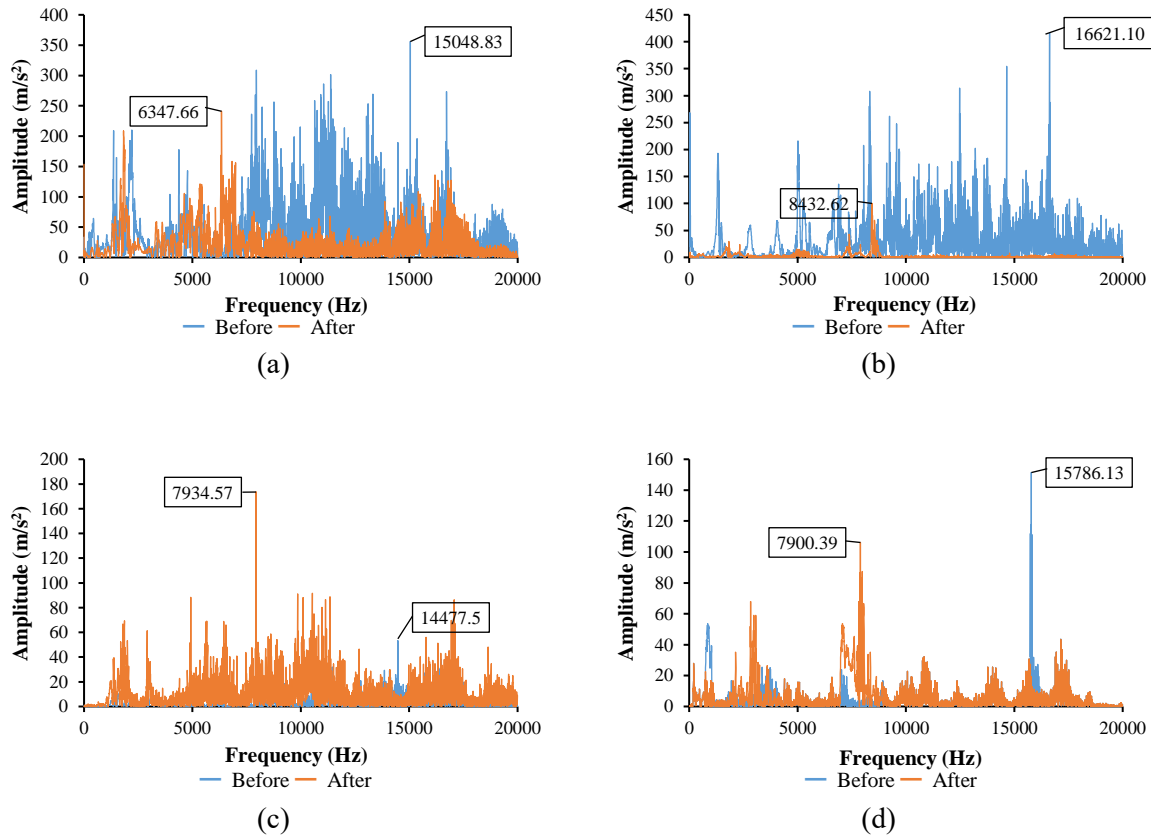


Fig. 11. Impact echo graph before and after corrosion SFB 8% A3.

The impact echo test results obtained the frequency values before and after accelerated corrosion. The frequency was selected because it represents the peak amplitude detected by the impact echo sensor within the signal window. The SFB test specimen has a higher frequency value than BN. The difference in frequency values can occur due to several factors, such as concrete density and the heterogeneous nature of the concrete mix [42]. SFB concrete has a higher average frequency value than BN, indicating that SFB has a better density than BN. The highest peak frequency value before corrosion was obtained by SFB 12% at 17323.0 Hz, while BN was 10214.8 Hz. After corrosion, the highest frequency was obtained by SFB 8% at a corrosion duration of 168 hours with a peak frequency of 7486.2 Hz, while BN was 2593.6 Hz. The frequency results show that SFB concrete has better concrete quality than BN. This is because SFB has a very fine size so that it can cover the pores in the concrete and make it denser. Fig 12 shows the relationship graph between the frequency value after corrosion and the corrosion level. The impact echo test results obtained show that the higher the corrosion level affects the frequency value. Frequency values will decrease as the corrosion rate increases [20]. In addition, cracks due to corrosion in the concrete cause the wave velocity to slow down and reduce the frequency value [42]. Therefore, the corrosion level will affect the specimen's frequency value, depending on the material used. The fine particles of SF will fill the concrete voids and make it denser, while the bacteria will help precipitate the calcite to fill the voids [12]. Therefore, BN has a lower frequency value than SFB. Based on the impact echo test results, the highest frequency values at 48 hours and 96 hours of accelerated corrosion duration were obtained by SFB 12% C1 and C2, while 168 hours were obtained by SFB 8% A3.

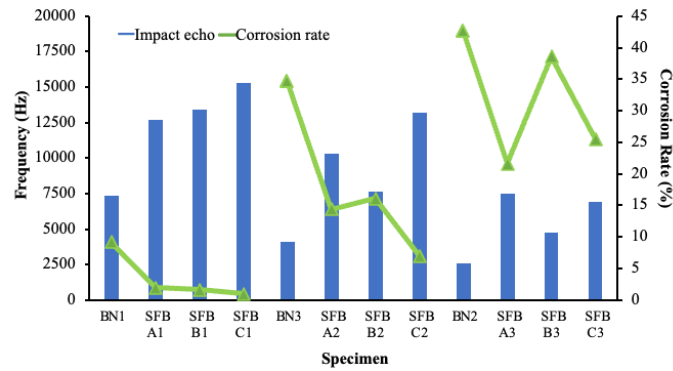


Fig. 12. Relationship between frequency value and corrosion rate.

3.3.2. Resistivity method

The resistivity testing method is utilized to ascertain the concrete's resistance to the corrosion of reinforcing steel. The resistivity value obtained from the test provides insights into the concrete's state and the likelihood of corrosion occurring in the reinforcing steel within the concrete. A higher resistivity of the concrete will result in a slower corrosion process. The resistivity of concrete when exposed to chloride indicates the likelihood of early corrosion damage. This is because low resistivity is consistently linked to swift chloride penetration [43]. A test was performed on concrete to assess its durability before and after corrosion. The study examined several types of silica fume concrete and the inclusion of extra microorganisms. Data was collected at four points, with two points left and right at the top and 2 points left and right at the bottom. The results of resistivity testing before corrosion in all BN and SFB specimens show resistivity values in the very low category. However, the resistivity value of normal concrete has a value that is far below SFB concrete as in SFB 12% C1 and BN1 has a difference of 20.24 kΩ.cm or 33.82% but still in the very low category in accordance with AASHTO TP 95 [30]. The resistivity results after being corroded decreased according to the duration of the corrosion. The resistivity value will decrease as the corrosion rate increases [20]. From the results obtained in the resistivity test after being corroded, the highest value at 48 and 96 hours of corrosion acceleration was received by the 12% SFB specimen at 41.81 kΩ.cm (very low) and 30.23 kΩ.cm (low), while at 168 hours it was obtained by 8% SFB with a value of 25.12 kΩ.cm (low). SFB concrete's resistivity value has better or better performance than normal concrete. SF concrete mixtures show good resistance to water permeation because the high specific surface area of SF will result in greater pozzolanic activity. Because its finer size is about 100 times finer than cement particles, it can fill the voids between particles and reduce the penetration of chloride ions [44]. SF concrete and added bacteria make the porosity of concrete smaller due to the small particle size of SF and the precipitation of calcite by bacteria [12]. Therefore, the resistivity value of SFB is higher or better than BN's. The resistivity value before corrosion and after corrosion can be seen in Fig 13. The graph shows that the higher the resistivity value, the lower the corrosion level, which means the value is inversely proportional.

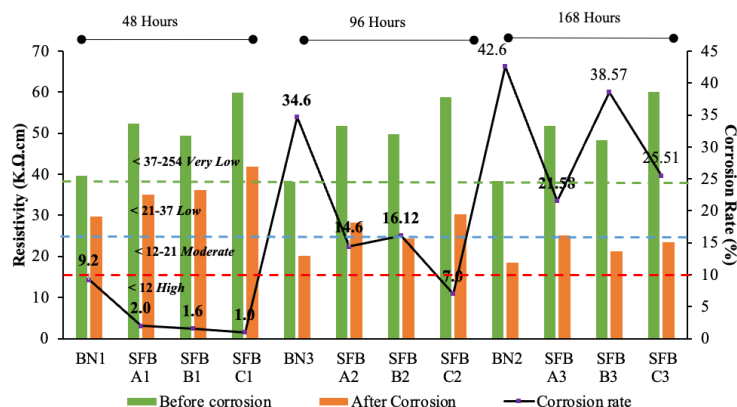


Fig. 13. Resistivity and corrosion rate relationship graph.

The resistivity value has a good correlation to the corrosion level, as can be seen in Fig 14 and Fig 15, which show a correlation value of $> 80\%$ in all specimens and $> 80\%$ for each separate specimen according to the variation. The relationship between resistivity and corrosion rate is linear, the graphs show that the higher the corrosion rate, the lower the resistivity value. This aligns with research by Zaki et al. [20], where the resistivity value will rise alongside the corrosion rate. When the corrosion rate of concrete increases, it leads to the deterioration of the material. Using resistivity tools, the assessment of concrete quality will be read according to the condition of the concrete.

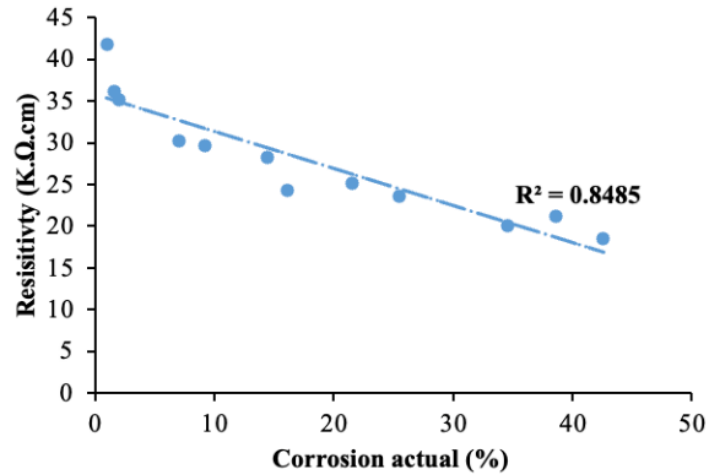


Fig. 14. The relationship between corrosion level and resistivity value.

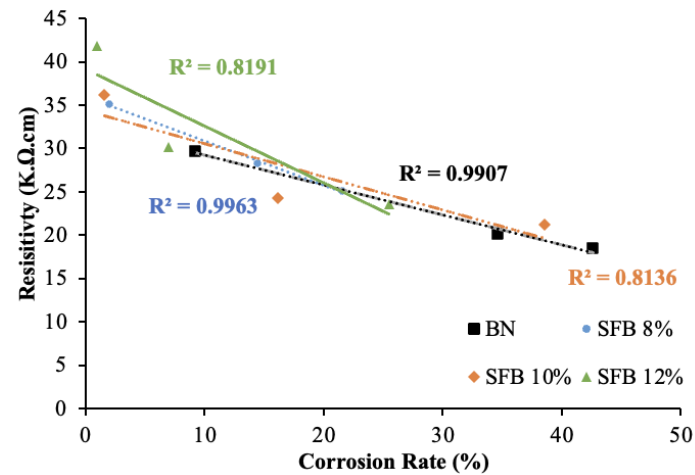


Fig. 15. Relationship between resistivity and corrosion rate with different corrosion duration.

3.4. Flexural strength

Testing the flexural strength of concrete is conducted following an accelerated corrosion process to assess the durability and strength of SFB concrete. Fig. 16 displays the results of the flexural strength test performed on the beam following corrosion. According to the flexural strength test findings, the highest values were observed in SFB, at 12%, after 48 hours and 96 hours of accelerated corrosion, with values of 18.45 MPa and 11.17 MPa, respectively. Regarding acceleration for 168 hours, SFB 8% showed a value of 7.07 MPa. BN has a lower flexural strength compared to SFB. As the level of corrosion increases, the adhesion between the concrete reinforcement will weaken. Corrosion has a significant impact on the mechanical properties of the reinforcement.

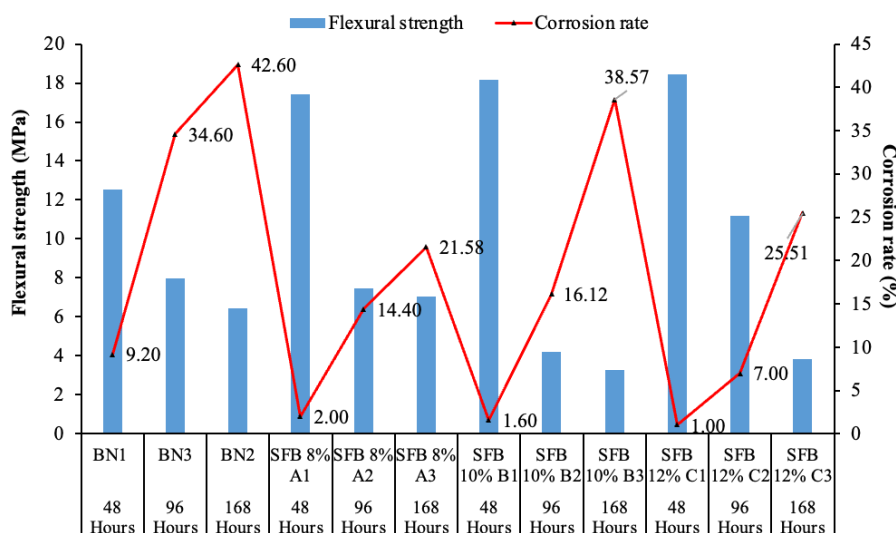


Fig. 16. Flexural strength data.

Additionally, the presence of corrosion products can lead to cracking and subsequent peeling of the surrounding concrete. When corrosion reaches severe levels, it can decrease the load-bearing capacity of structural components [39,45]. Thus with its higher corrosion rate than SFB, BN exhibits a lower flexural strength value. The correlation between the corrosion rate and flexural strength value is clear in Fig. 17. Aside from considering corrosion factors, including SF and bacteria in the specimens can enhance flexural strength. Adding SF to concrete can enhance its flexural strength [46]. The addition of *Bacillus subtilis* bacteria to concrete will increase its flexural strength due to calcite deposits by these bacteria.

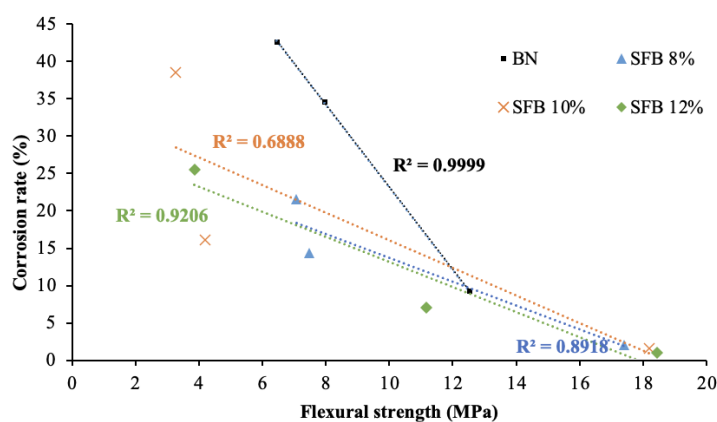


Fig. 17. Relationship between flexural strength and corrosion rate.

3.5. Concrete failure pattern

Based on SNI 1974-2011, there are five different patterns of destruction in cylindrical concrete. These include cone destruction, cone and split destruction, cone and shear destruction, shear destruction, and upright axis parallel destruction [47]. The difference in crack patterns can occur due to the inhomogeneous distribution of coarse aggregates in the concrete mixture, which causes cracks to occur at points that are less filled with aggregates. Besides differences in crack patterns can also occur due to the segregation or separation of concrete materials during the manufacture of test specimens [48]. In Fig 18, the cylindrical concrete shows shear cone destruction. The cracks that occur in each test specimen mostly have the same crack pattern. The addition of 10% SFB has the same destruction pattern in all specimens, but the destruction is more severe than in others. SFB 10% has a lower compressive strength value than other test specimens, while BN has less destruction. BN is more homogeneous, and its aggregate distribution is even greater than that of SFB.

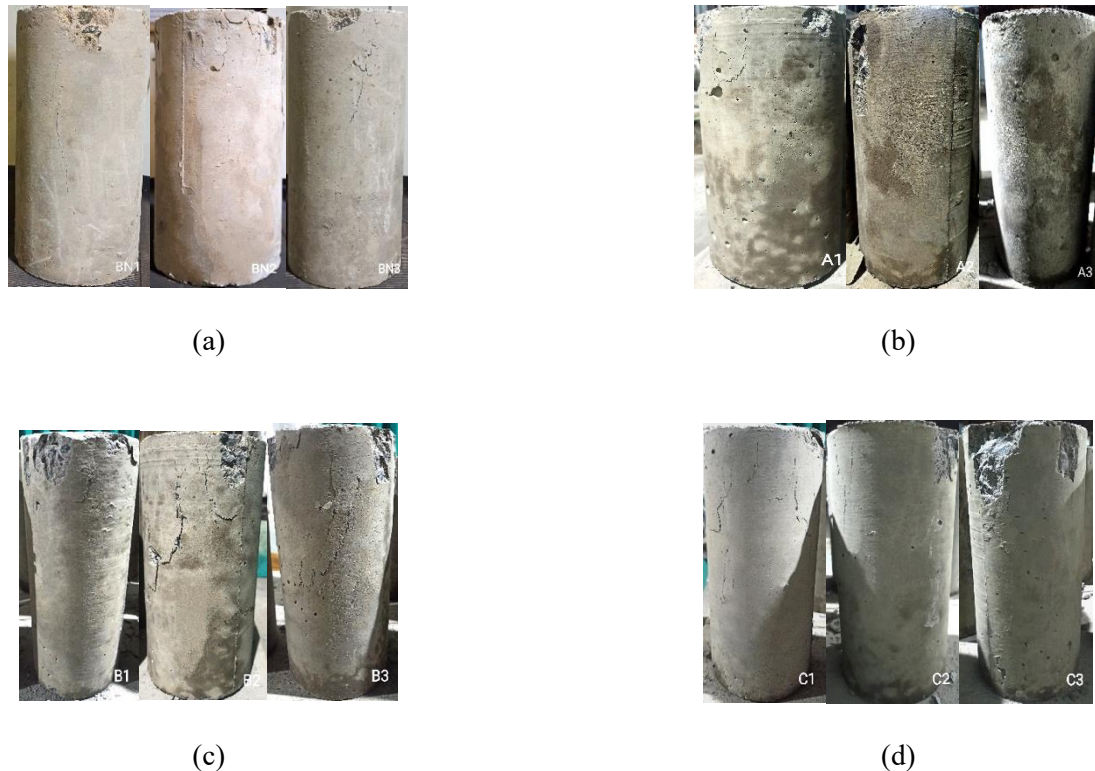
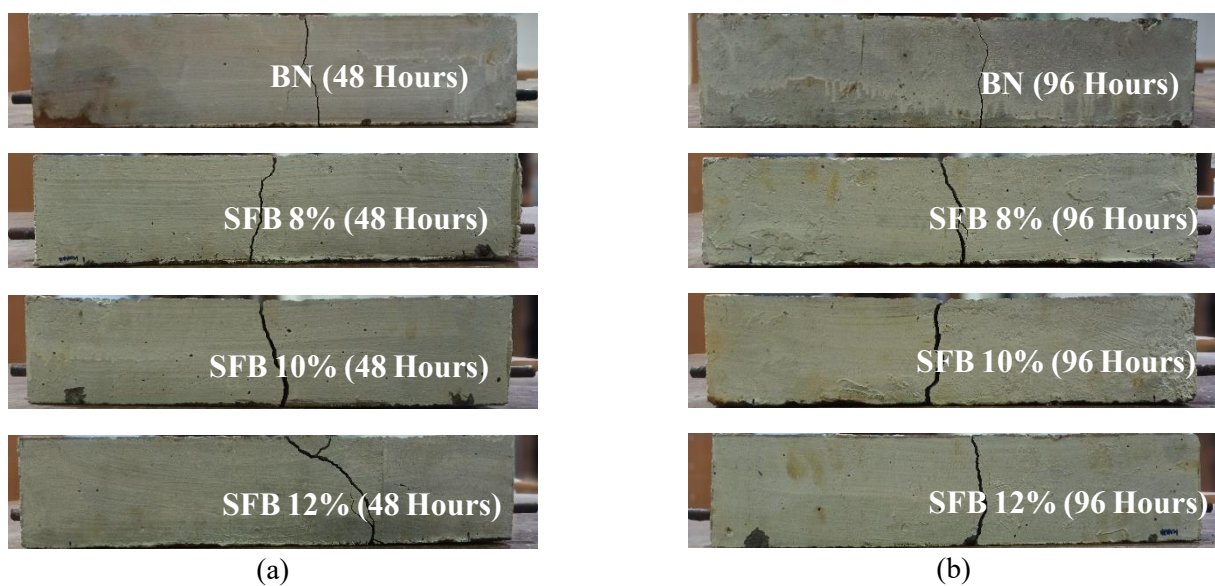


Fig. 18. Failure pattern of cylindrical concrete (a) BN, (b) SFB 8%, (c) SFB 10%, and (d) SFB 12%.

Testing the flexural strength of the beam specimens after being corroded, there are crack patterns from different test specimens and different corrosion acceleration durations. Cracks in the span's center can be interpreted as flexural cracks [49]. Based on the results of the flexural strength test, all specimens fall into the flexural cracking category, as can be seen in Fig 19. The higher the level of corrosion in the concrete block, the smaller the cracks formed, which indicates the lower bonding properties of the concrete block. The lower bonding properties are due to the corrosion products (rust) releasing pressure, resulting in more cracking and peeling of the bonding area, so the tensile force is reduced, and the number of cracks is also reduced [43]. Therefore, the cracks in the BN specimen have a flexural failure pattern with smaller cracks.



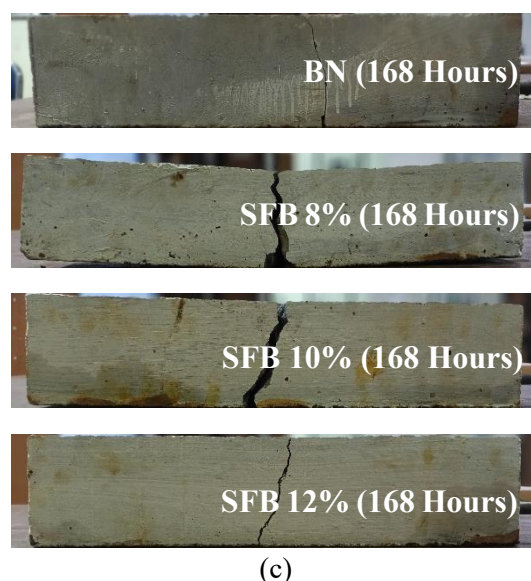


Fig. 19. Flexural strength test results (a) 48 hours, (b) 96 hours, and (c) 168 hours.

3.6. Relationship between impact echo and resistivity values

Observing the relationship between resistivity and impact echo testing is crucial in determining the correlation between these two factors and corrosion in concrete. Fig. 20 displays the correlation values of resistivity and impact echo methods, with a value of 0.948 before corrosion and 0.8878 after. The relationship between impact echo and resistivity testing methods indicates a strong correlation in assessing concrete condition before and after corrosion.

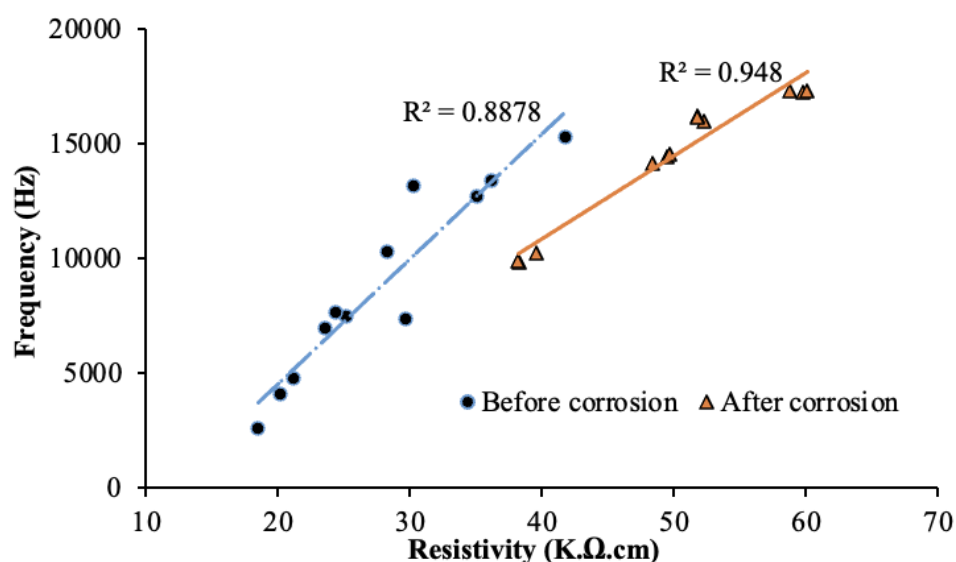


Fig. 20. Relationship between resistivity and impact echo values.

Fig 21 shows the relationship between the impact echo and resistivity values to the corrosion rate. The relationship between impact echo and resistivity values to the corrosion rate strongly correlates above 80%. This shows that impact echo and resistivity testing can assess corrosion levels well. The higher the corrosion rate, the lower the impact echo and resistivity values. Resistivity has a better relationship with the corrosion rate than impact echo. This indicates that resistivity values are better at assessing corroded concrete.

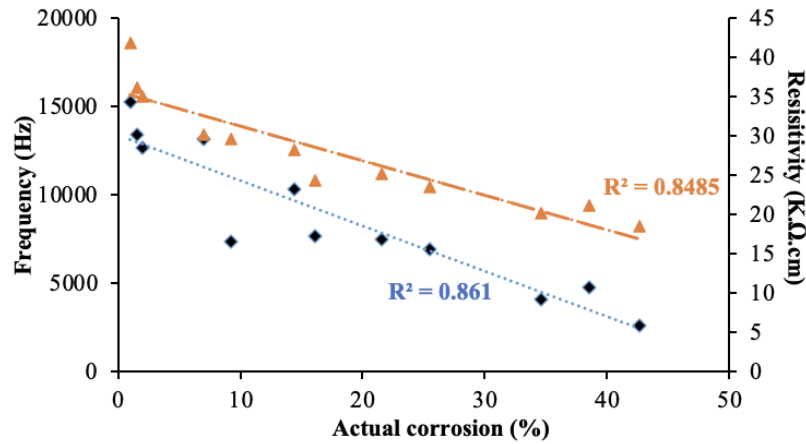


Fig. 21. Relationship of impact echo and resistivity values to corrosion rate.

Fig 22 illustrates the correlation between impact echo and resistivity to flexural strength, as a significant level of corrosion can greatly impact the concrete's strength. The correlation between impact echo and flexural strength is over 90%, except for SFB 8%. On the other hand, the resistivity to flexural strength is over 90% for all test objects. This shows that impact echo and resistivity testing can accurately predict the flexural strength value of corroded concrete. SFB 8% in the impact echo relationship with flexural strength only has a correlation value of 0.7382. This is because from testing the flexural strength of SFB 8% on specimens A2 and A3, the flexural strength is almost the same with a difference of only 0.42 MPa. This results in SFB 8% not having linear results. The relationship between the resistivity value and flexural strength has a stable correlation, namely >90%, which means that the quality of the concrete can be seen or evaluated using a resistivity tool properly.

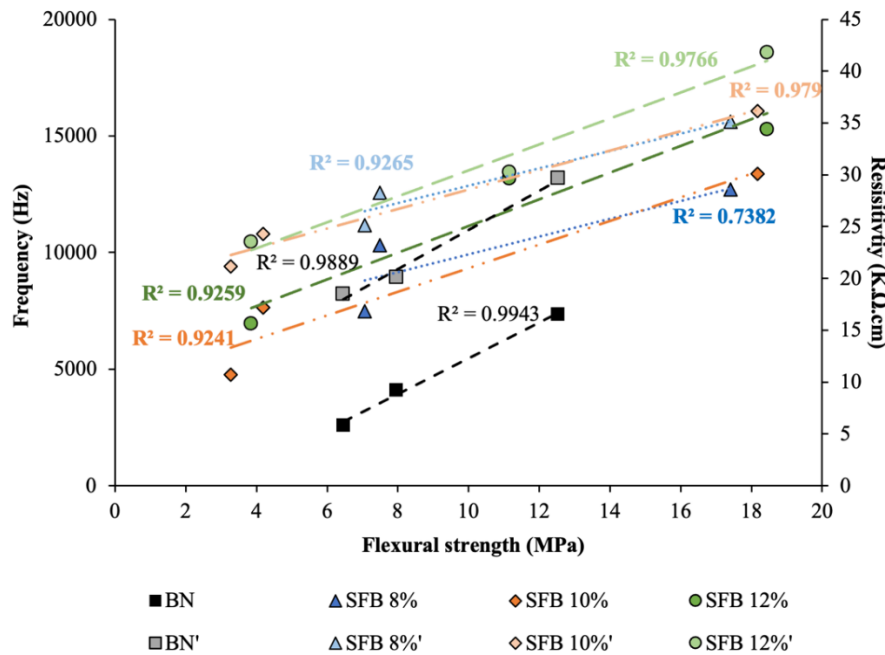


Fig. 22. Relationship of impact echo and resistivity values to flexural strength.

3.7. Self-healing

Once the accelerated corrosion process is finished, the self-healing test involves spraying water on the cracked concrete. This activates the bacteria, allowing them to cover the cracks. The self-healing process will begin when water (H₂O) enters the crack and reacts with the bacteria [50]. Visual observations were made for 28 days, and observation data was taken every 7 days to see the development of bacteria covering

the cracks. In the self-healing process of 28 days, it was found that all specimens with bacteria-added materials were not covered completely. The high pH of the cement can allow bacterial cells to grow slowly in the initial period and adapt to high pH conditions in the curing period. In addition, bacterial cells may be damaged or die. In addition to the pH factor, the crack width in the specimen also affects the performance of bacteria towards crack closure [51]. The effective crack width that bacteria can close is 0.3 mm, and the development of bacteria can be inhibited because the concrete surface has a low pH due to carbonation. In contrast, the pH in the concrete has a high value. As a result, the healing rate decreases dramatically with the increase in crack area [52]. This results in the bacteria not working properly. However, the spores of *Bacillus subtilis* bacteria can survive in concrete for up to 200 years, which will activate when exposed to water and oxygen [53–55]. Of all the specimens added with *Bacillus subtilis* bacteria, only specimen SFB 12% C2 appeared to a bacteria, although it did not cover it completely. However, this indicates that bacteria can survive in extreme environments. The appearance of bacteria can be seen in Fig 23.

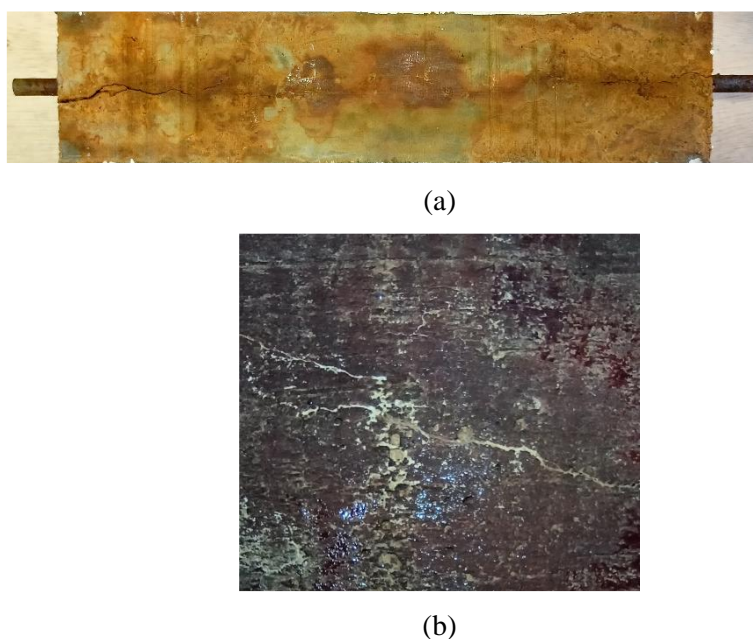


Fig. 23. The appearance of bacteria on the specimen (a) 12% SFB test piece and (b) Detail of 12% SF C2.

4. Conclusions

Based on the research experiment, the analysis of the results reveals some interesting findings regarding the evaluation of silica fume on the self-healing performance of corroded concrete using the NDT method. From these findings, certain conclusions can be drawn:

- The compressive strength of SFB concrete is lower than that of BN concrete. This reduction is primarily due to the water-absorbing nature of silica fume (SF), which decreases the workability of the mix and negatively affects strength development. The recorded compressive strengths were 37.59 MPa for BN, 33.99 MPa for SFB 8%, 24.10 MPa for SFB 10%, and 29.92 MPa for SFB 12%. The addition of silica fume and bacteria enhances the concrete's resistance to chloride ion penetration, as evidenced by lower current values observed during accelerated corrosion testing. The results of flexural strength tests performed post-accelerated corrosion indicate a reduction in flexural strength, which correlates with the increasing rate of corrosion..
- The collapse pattern of the SFB 10% cylindrical concrete specimen was more severe than that of the other specimens, likely due to the uneven distribution of coarse aggregate. Additionally, the crack patterns observed in all concrete specimens exhibited characteristics typical of flexural failure. The impact echo and resistivity values are inversely proportional to the corrosion rate. The higher corrosion

rate results in lower impact echo and resistivity frequency values. At a corrosion rate of around 10%, the impact echo value is 7500 Hz, and the resistivity is $30 \text{ k}\Omega \cdot \text{cm}$. As the corrosion level increases to around 30%, the impact echo decreases to 5000 Hz, and the resistivity drops to $20 \text{ k}\Omega \cdot \text{cm}$. This data demonstrates a clear relationship between the corrosion rate and both the impact echo and resistivity value. The impact echo and resistivity methods have higher effectiveness in evaluating concrete that has the potential for corrosion and concrete that has been exposed to the effects of corrosion.

- With the use of silica fume and *Bacillus subtilis* bacteria additives, concrete becomes more resistant to chloride ion penetration, which is the primary factor that initiates reinforcement corrosion. This resistance helps in preventing the onset of corrosion within the reinforcement, thereby enhancing the durability of the structure. As a result, incorporating silica fume and *Bacillus subtilis* bacteria additives significantly improves the service life and overall performance of reinforced concrete in construction buildings. This combination not only strengthens the concrete matrix but also helps in mitigating long-term maintenance issues caused by corrosion. Further research is required, particularly regarding the microstructure of SFB concrete, to better understand the ongoing development of bacteria for self-healing properties. Additionally, it is essential to investigate the formation of C-S-H (calcium silicate hydrate) in SFB concrete, as this compound plays a crucial role in enhancing the concrete's strength. Understanding these aspects will provide valuable insights into the long-term performance of SFB concrete and its potential for improving the durability and sustainability of reinforced concrete structures.

Funding

The research was funded through a grant scheme by Universitas Muhammadiyah Yogyakarta Fiscal Year 2023/2024 with grant number 50/R-LRI/XII/2023.

Conflicts of interest

The authors declare that they have no known competing financial interests or personal relationships that could have appeared to influence the work reported in this paper.

Authors contribution statement

Ahmad Zaki: Conceptualization; Methodology; Formal analysis; Writing – review & editing.

Muhammad Restu Riady Putra: Investigation Data curation; Roles/Writing – original draft.

Sri Atmaja P. Rosyidi: Resources; Software; Supervision; Validation.

Abdullah M. Zeyad: Supervision; Validation; Writing – review & editing.

Kharisma Wira Nindhita: Project administration; Roles/Writing – original draft.

References

- [1] Wasim M, A.A A, Abu B, Alshaikh I. Future Directions for the Application of Zero Carbon Concrete in Civil Engineering- A Review. *Case Stud Constr Mater* 2022;17:e01318. <https://doi.org/10.1016/j.cscm.2022.e01318>.
- [2] Zamba DD, Mohammed TA. Self-healing performance of normal strength concrete with *Bacillus subtilis* bacteria. *J Build Pathol Rehabil* 2023;9:4. <https://doi.org/10.1007/s41024-023-00356-5>.
- [3] Hashmi A, Khan M, Bilal M, Shariq M, Baqi A. Green Concrete: An Eco-Friendly Alternative to the OPC Concrete. *CONSTRUCTION* 2022;2:93–103. <https://doi.org/10.15282/construction.v2i2.8710>.

- [4] Nafees A, Amin M, Khan K, Nazir K, Ali M, Javed MF, et al. Modeling of Mechanical Properties of Silica Fume-Based Green Concrete Using Machine Learning Techniques. *Polymers (Basel)* 2021;14:30. <https://doi.org/10.3390/polym14010030>.
- [5] ACI-Committee-234. ACI 234R-06 R12 Guide for the Use of Silica Fume in Concrete_MyCivil.ir. Guid Use Silica Fume Concr 2006.
- [6] Zaki A, Husnah. Evaluation of fly ash concrete in salt environment. *E3S Web Conf* 2023;429. <https://doi.org/10.1051/e3sconf/202342905030>.
- [7] Rahita A, Zaki A. Corrosion Analysis on Reinforcing Steel in Concrete Using the Eddy Current Method. 2023. <https://doi.org/10.1109/ICE3IS59323.2023.10335487>.
- [8] Patil A. Study of Influence of Corrosion and Cracking on Bond Behavior of Reinforced Concrete Member. *J Struct Eng Manag* 2017;4:58–67.
- [9] Ghewa G. Efek Penggunaan Supplementary Material Pada Beton, Ditinjau Terhadap Susut Dan Induksi Keretakan Akibat Korosi. *J Rekayasa Konstr Mek Sipil* 2022;5:61–7. <https://doi.org/10.54367/jrkms.v5i2.2001>.
- [10] Hussein ZM, Abedali AH, Ahmead AS. Improvement Properties of Self -Healing Concrete by Using Bacteria. *IOP Conf Ser Mater Sci Eng* 2019;584:12034. <https://doi.org/10.1088/1757-899X/584/1/012034>.
- [11] Ha Nguyen T, Ghorbel E. Effects of *Bacillus Subtilis* on the Compressive Strength, Porosity and Rapid Chloride Permeability of Concrete. *AJCE - Spec Issue* 2019;37:223–8.
- [12] Siddique R, Jameel A, Singh M, Barnat-Hunek D, Kunal, Ait-Mokhtar A, et al. Effect of bacteria on strength, permeation characteristics and micro-structure of silica fume concrete. *Constr Build Mater* 2017;142:92–100. <https://doi.org/https://doi.org/10.1016/j.conbuildmat.2017.03.057>.
- [13] Rashidi A, Zain S, Ahmadi R. Mix proportion for medium grade concrete with silica fume as cement replacement for general purpose construction. *IOP Conf Ser Mater Sci Eng* 2021;1101:12013. <https://doi.org/10.1088/1757-899X/1101/1/012013>.
- [14] Škuldeckė J, Vaitkus A, Šernas O, Čygas D. Effect of Silica Fume on High-strength Concrete Performance. 2020. <https://doi.org/10.11159/icsect20.162>.
- [15] Prayuda H, Soebandono B, Cahyati MD, Monika F. Repairing of Flexural Cracks on Reinforced Self-Healing Concrete Beam using *Bacillus Subtillis* Bacteria. *Int J Integr Eng* 2020;12:300–9. <https://doi.org/10.30880/ijie.2020.12.04029>.
- [16] Nindhita KW, Zaki A. State of the art: Correlation self-healing agent and corrosion on concrete. *E3S Web Conf* 2023;429. <https://doi.org/10.1051/e3sconf/202342905034>.
- [17] Aswin M, Andres, Gotami R. Studies on Strength and Flexural Behaviour of Reinforced Concrete Beams with the Corroded Steel Reinforcements as a result of Sodium Chloride (NaCl). *J Phys Conf Ser* 2023;2421:12029. <https://doi.org/10.1088/1742-6596/2421/1/012029>.
- [18] Mahbubi K, Zaki A, Nugroho G. Bibliometric and Scientometric Trends in Structural Health Monitoring Using Fiber-Optic Sensors: A Comprehensive Review. *J Civ Hydraul Eng* 2024;2:51–64. <https://doi.org/10.56578/jche020104>.
- [19] Karla H, Danner T, Geiker M. Non-destructive Test Methods for Corrosion Detection in Reinforced Concrete Structures. *Nord Concr Res* 2020;62:41–61. <https://doi.org/10.2478/ncr-2019-0005>.
- [20] Zaki A, Fikri M, Wibisono C, Rosyidi SAP. Evaluating Pre-Corrosion and Post-Corrosion of Oil Palm Shell Concrete with Non-Destructive Testing. *Key Eng Mater* 2023;942:137–62. <https://doi.org/10.4028/p-9qfaiq>.
- [21] Badan Standarisasi Nasional. Metode uji untuk analisis saringan agregat halus dan agregat kasar. 2012.
- [22] SNI 1970. Cara Uji Berat Jenis dan Penyerapan Air Agregat Halus. *Badan Standar Nas Indones* 2008:7–18.
- [23] Indonesia SN, Nasional BS. Metode uji bahan yang lebih halus dari saringan 75 μ m (No. 200) dalam agregat mineral dengan pencucian (ASTM C117–2004, IDT) ICS 2004.
- [24] Badan Standarisasi Nasional. Metode uji berat jenis dan penyerapan agregat kasar. 2016.
- [25] Standar Nasional Indonesia Cara uji keausan agregat dengan mesin abrasi Los Angeles n.d.
- [26] ACI Committee. Standard Practice for Selecting Proportions for Normal, Heavyweight, and Mass Concrete (ACI 211.1-91) Chairman, Subcommittee A. 1991.
- [27] SNI 2493:2011. SNI 2493:2011 Tata Cara Pembuatan dan Perawatan Benda Uji Beton di Laboratorium. *Badan Standar Nas Indones* 2011:23.

- [28] Mulyati M, Arkis Z. Pengaruh Metode Perawatan Beton Terhadap Kuat Tekan Beton Normal. *J Tek Sipil ITP* 2020;7:78–84. <https://doi.org/10.21063/jts.2020.v702.05>.
- [29] Zaki A, Ying T, Chai HK, Aggelis D. Assessment of Corrosion Damage using Acoustic Emission Technique under Load Testing. 2015.
- [30] AASHTO. Aashto-Tp-95-14 n.d.
- [31] Aslam M, Shafigh P, Jumaat MZ, Bhosale A, Zade NP, Sarkar P, et al. iTeh Standards iTeh Standards Document Preview. *Nanomaterials* 2022;126:13–5. <https://doi.org/10.1520/C1383-15.10.1520/C1383-15R22>.
- [32] Nindhita KW, Zaki A, Zeyad AM. Effect of Bacillus Subtilis Bacteria on the mechanical properties of corroded self-healing concrete. *Frat Ed Integrita Strutt* 2024;18:140–58. <https://doi.org/10.3221/IGF-ESIS.68.09>.
- [33] Haynes GS, Baboian R. Laboratory Corrosion Tests and Standards 1985. <https://doi.org/10.1520/STP866-EB>.
- [34] Badan Standarisasi Nasional. Cara Uji Kuat Tekan Beton dengan Benda Uji Silinder. 2011.
- [35] SNI 4154-2014. Metode Uji Kekuatan Lentur Beton (Menggunakan Balok Sederhana dengan Beban Terpusat di Tengah Bentang). Badan Standar Nas Indones 2014:1–12.
- [36] Arman A, Nugroho F, Mulyati M, Azman F. PENGARUH PENAMBAHAN SILIKA FUME TERHADAP KUAT TEKAN BETON. *J Teknol Dan Vokasi* 2023;2:9–16. <https://doi.org/10.21063/jtv.2024.2.1.2>.
- [37] Wolo D, Ngapa YD, Carvallo L. Potensi Zeolit Alam Ende Sebagai Bahan Aditif Semen Untuk Meningkatkan Kuat Tekan Beton. *Opt J Pendidik Fis* 2019;3:34–41.
- [38] Sutriyono B, Trimurtiningrum R, Rizkiardi A. Pengaruh Silica Fume sebagai Substitusi Semen terhadap Nilai Resapan dan Kuat Tekan Mortar (Hal. 12-21). *RekaRacana J Tek Sipil* 2018;4:12. <https://doi.org/10.26760/rekaracana.v4i4.12>.
- [39] Kearsley E, Joyce A. Effect of corrosion products on bond strength and flexural behaviour of reinforced concrete slabs. *J South African Inst Civ Eng* 2014;56:21–9.
- [40] Dacuan C, Abellana V, Canseco-Tuñacao HA. Mechanical Properties of Corroded-Damaged Reinforced Concrete Pile-supporting Wharves. *Civ Eng J* 2020;6:2375–96. <https://doi.org/10.28991/cej-2020-03091624>.
- [41] Sharkawi A, Seyam A. Efficiency of accelerated techniques for assessing corrosion protection of blended cements. *Mag Concr Res* 2018;71:637–46. <https://doi.org/10.1680/jmacr.17.00269>.
- [42] Alhawati M, Khan A, Ashour A. Evaluation of Steel Corrosion in Concrete Structures Using Impact-Echo Method. *Adv Mater Res* 2020;1158:147–64. <https://doi.org/10.4028/www.scientific.net/AMR.1158.147>.
- [43] Zaki A, Chai HK, Aggelis DG, Alver N. Non-Destructive Evaluation for Corrosion Monitoring in Concrete: A Review and Capability of Acoustic Emission Technique. *Sensors* 2015;15:19069–101. <https://doi.org/10.3390/s150819069>.
- [44] Chaudhary S, Sinha A. Effect of Silica Fume on Permeability and Microstructure of High Strength Concrete. *Civ Eng J* 2020;6:1697–703. <https://doi.org/10.28991/cej-2020-03091575>.
- [45] Patil A. Influence of Corrosion on Flexural Strength of Concrete. *J Struct Eng Manag* 2017;4:35–42.
- [46] Matlab T, Breesem K, Hassen D, Jaafar A. Stress-strain behaviour and flexural strength of silica fume polymer-modified concrete. *IOP Conf Ser Mater Sci Eng* 2020;881:12167. <https://doi.org/10.1088/1757-899X/881/1/012167>.
- [47] Cara uji kuat tekan beton dengan benda uji silinder Badan Standardisasi Nasional 2011.
- [48] Zaki A, Pratama TY, Wibisono CA, Saleh F. Pengaruh Cks Sebagai Pengganti Agregat Pada Kuat Tekan Beton. *J Ris Rekayasa Sipil* 2023;6:119. <https://doi.org/10.20961/jrrs.v6i2.69039>.
- [49] Aqli K, S E, Wisnumurti W. Pengaruh Limbah Batu Onyx Pengganti Agregat Kasar Beton Terhadap Pola Retak Balok Beton Bertulang. *CRANE Civ Eng Res J* 2021;2:33–8. <https://doi.org/10.34010/crane.v2i1.5014>.
- [50] C. N. Application of Bacillus Subtilis Bacteria for Improving Properties and Healing of Cracks in Concrete. *Int J Adv Res Trends Eng Technol* 2018;5:118. <https://doi.org/10.20247/IJARTET.2018.05S05030023>.
- [51] Vijay K, Murmu M, Deo S. Bacteria based self healing concrete – A review. *Constr Build Mater* 2017;152:1008–14. <https://doi.org/10.1016/j.conbuildmat.2017.07.040>.
- [52] Feng J, Chen B, Sun W, Wang Y. Microbial induced calcium carbonate precipitation study using Bacillus subtilis with application to self-healing concrete preparation and characterization. *Constr Build Mater* 2021;280:122460. <https://doi.org/10.1016/j.conbuildmat.2021.122460>.

- [53] Manvith Kumar Reddy C, Ramesh B, Macrin D, Reddy K. Influence of bacteria *Bacillus subtilis* and its effects on flexural strength of concrete. *Mater. Today Proc.*, vol. 33, Elsevier Ltd; 2020, p. 4206–11. <https://doi.org/10.1016/j.matpr.2020.07.225>.
- [54] Priyom SN, Ismal MM, Shumi W. Assessment on strength characteristics of microbial concrete by using *bacillus subtilis* as self-healing agent: A critical review. *Int J Sustain Constr Eng Technol* 2020;11:34–44. <https://doi.org/10.30880/ijscet.2021.11.04.004>.
- [55] Stanaszek-Tomal E. Bacterial Concrete as a Sustainable Building Material? *Sustainability* 2020;12. <https://doi.org/10.3390/su12020696>.